

## CORONAVIRUS

# Serial interval of SARS-CoV-2 was shortened over time by nonpharmaceutical interventions

Sheikh Taslim Ali<sup>1\*</sup>, Lin Wang<sup>2,3\*</sup>, Eric H. Y. Lau<sup>1\*</sup>, Xiao-Ke Xu<sup>4</sup>, Zhanwei Du<sup>5</sup>, Ye Wu<sup>6,7</sup>, Gabriel M. Leung<sup>1</sup>, Benjamin J. Cowling<sup>1†</sup>

Studies of novel coronavirus disease 2019 (COVID-19), which is caused by severe acute respiratory syndrome coronavirus 2 (SARS-CoV-2), have reported varying estimates of epidemiological parameters, including serial interval distributions—i.e., the time between illness onset in successive cases in a transmission chain—and reproduction numbers. By compiling a line-list database of transmission pairs in mainland China, we show that mean serial intervals of COVID-19 shortened substantially from 7.8 to 2.6 days within a month (9 January to 13 February 2020). This change was driven by enhanced nonpharmaceutical interventions, particularly case isolation. We also show that using real-time estimation of serial intervals allowing for variation over time provides more accurate estimates of reproduction numbers than using conventionally fixed serial interval distributions. These findings could improve our ability to assess transmission dynamics, forecast future incidence, and estimate the impact of control measures.

In December 2019, a novel coronavirus disease [coronavirus disease 2019 (COVID-19)], caused by severe acute respiratory syndrome coronavirus 2 (SARS-CoV-2), was first reported in Wuhan, China. It has since spread to more than 212 countries, causing more than 10 million confirmed cases and 500,000 deaths worldwide as of 30 June 2020 (1). Recent studies have suggested that several demographic and social factors can influence the transmission of COVID-19, including age- and gender-related differences in infection risk (2–4), reduced risk of infection as a result of intensive nonpharmaceutical interventions (NPIs) (e.g., isolation and social distancing) (5–7), and abrupt changes in social mixing patterns because of lockdowns and confinement (8–10). Serial interval, defined as the duration between the symptom-onset time of the infector and that of the infectee, is an essential metric for estimating many other key epidemiological parameters (e.g., reproduction number, generation time, and attack rate), which are used in turn to predict disease trends and health care demands (11). In early studies, before the availability of specific data on COVID-19, the serial interval distribution of COVID-19 was assumed to be similar to those of severe acute respiratory syndrome (SARS) or Middle East respiratory syndrome (MERS), with a mean >8 days (12, 13). Once specific data became available on COVID-19 transmission pairs, several studies examined the serial interval distribution of COVID-19 in different locations, with estimates of the mean

serial interval varying from 3.1 to 7.5 days (6, 14–21). All of these studies have assumed that the timing of transmission events can be described by a single, stable distribution of serial intervals at different stages of an epidemic.

In fact, the serial interval depends on the incubation period, the profile of infectiousness after infection, and the variation in contact structure of the population (as explained in fig. S1) (22). The incubation period describes the biological process of disease progression and tends to follow a more similar distribution from one location to another, with minor variations resulting from social or cultural differences in how symptoms are perceived or reported. However, the profile of infectiousness over time can vary because of human behavior. Changes in contact patterns and the use of public health measures can reshape the timing of infection events by limiting successful contacts overall (e.g., social distancing) or after illness onset (e.g., case isolation). Interventions such as the isolation of confirmed and suspected cases, suspension of intra- and intercity travel, and different forms of social distancing were widely implemented in different Chinese cities. This provides an opportunity to study the temporal changes in the serial interval distribution and its association with NPIs. Here, we show that variation in the serial interval can occur and has important implications for the assessment of transmission dynamics and the impact of control measures.

We compiled a database of 1407 COVID-19 transmission pairs, in which symptom-onset dates and social relationships were available for both the infector and infectee of 677 transmission pairs [see table S1 for entire database (23) and supplementary materials for details]. Household and nonhousehold transmissions were identified on the basis of the information on social relationships (e.g., familial members of the same household, non-household relatives, colleagues, classmates, friends, and other face-to-face contacts). The data were reconstructed from the publicly available reports of 9120 confirmed COVID-19 cases reported by 27 provincial and 264 urban health commissions in China outside Hubei province. Data from Hubei province were excluded because there was less reliable information on chains of transmission during the widespread community circulation of COVID-19; outside Hubei province, it was more straightforward to link connected cases and derive serial intervals. We focused on 677 transmission pairs with infectors having developed symptoms from 9 January through 13 February 2020. This 36-day period spans a series of key interventions related to the evolving epidemiology and transmission dynamics of COVID-19 in mainland China (24–26).

We first calculated the number of transmission pairs in our database by the onset dates of infectors (fig. S3). Because many infectors (339) developed symptoms during 23 to 29 January 2020, we defined this 1-week period as the peak week, the previous 14-day period (9 to 22 January 2020) as the prepeak period, and the following 15-day period (30 January to 13 February 2020) as the postpeak period. We computed the serial interval as the number of days between the symptom-onset date of the infector and that of the infectee for each transmission pair. Empirical serial interval distributions for transmission pairs, counting from symptom onsets of the infectors during each period, indicate that the serial intervals shortened over time (Fig. 1A).

We estimated the serial interval distribution during each nonoverlapping period by fitting a normal distribution to the corresponding serial intervals data (supplementary materials). Analysis of all 677 transmission pairs revealed that the serial interval distribution had a mean of 5.1 [95% credibility interval (CrI): 4.7, 5.5] days and a standard deviation (SD) of 5.3 (95% CrI: 5.0, 5.6) days (table S2) overall, which is consistent with other recent

<sup>1</sup>WHO Collaborating Centre for Infectious Disease Epidemiology and Control, School of Public Health, Li Ka Shing Faculty of Medicine, The University of Hong Kong, Hong Kong Special Administrative Region, China. <sup>2</sup>Department of Genetics, University of Cambridge, Cambridge CB2 3EH, UK. <sup>3</sup>Mathematical Modelling of Infectious Diseases Unit, Institut Pasteur, UMR2000, CNRS, Paris 75015, France. <sup>4</sup>College of Information and Communication Engineering, Dalian Minzu University, Dalian 116600, China. <sup>5</sup>Department of Integrative Biology, University of Texas at Austin, Austin, TX 78705, USA. <sup>6</sup>School of Journalism and Communication, Beijing Normal University, Beijing 100875, China. <sup>7</sup>Computational Communication Research Center, Beijing Normal University, Zhuhai 519087, China.

\*These authors contributed equally to this work.  
†Corresponding author. Email: bcowling@hku.hk

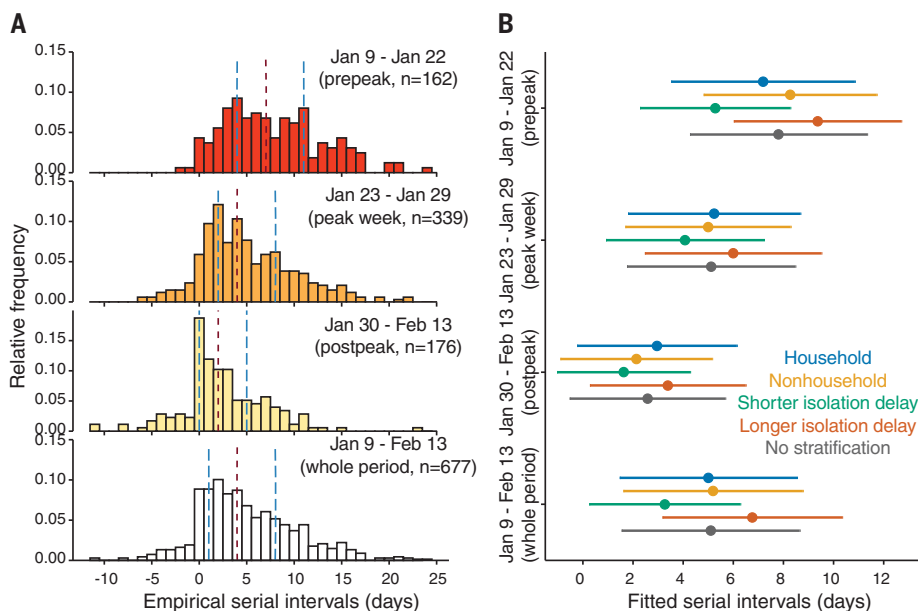


**Fig. 1. Serial intervals of SARS-CoV-2 substantially shortened over time in mainland China.** (A) Empirical serial interval distributions. From top to bottom, transmission pairs were analyzed by selecting infectors who developed symptoms during 9 to 22 January 2020 (prepeak); 23 to 29 January 2020 (peak week); 30 January to 13 February 2020 (postpeak); and 9 January to 13 February 2020 (whole period), respectively. In each panel, vertical dashed lines in red and blue colors indicate the median and interquartile range (IQR), respectively. (B) Estimated serial interval distributions by fitting a normal distribution using MCMC. From top to bottom, each group of bars corresponds to the transmission pairs with infectors who developed symptoms during the prepeak (162 pairs), peak week (339 pairs), postpeak (176 pairs), and whole 36-day period (677 pairs), respectively. Colored dots and bars correspond to the transmission pairs within households (blue), outside households (yellow), with isolation delays shorter than the median isolation delay of each period (green), and with isolation delays longer than the median isolation delay of each period (orange), respectively. Dark gray bars correspond to transmission pairs with no stratification. Dots and bars indicate the estimated median and IQR, respectively.

studies (16, 21, 27). However, fitting to data of nonoverlapping periods of time revealed considerable variation in serial interval distributions (Fig. 1B). Before the peak, the mean and SD of serial intervals were estimated to be 7.8 (7.0, 8.6) days and 5.2 (4.7, 5.9) days, respectively. During the peak, the mean and SD reduced to 5.1 (4.6, 5.7) days and 5.0 (4.6, 5.4) days, respectively. After the peak, these estimates further shortened to 2.6 (1.9, 3.2) days and 4.6 (4.2, 5.1) days, respectively (table S2).

Next, we examined the real-time change in serial intervals by using a series of running time windows with fixed lengths of 10, 14, or 18 days (fig. S10). In contrast to the use of a constant distribution of serial intervals, our analysis suggests that serial intervals were gradually shortened over the study period (Fig. 2A), which is robust to alternative specifications of time windows (fig. S10). By fitting the transmission pairs data for each running time window by Markov chain Monte Carlo (MCMC) (Fig. 2A and table S3), we estimated that during the first 14-day period (9 to 22 January 2020), the serial intervals were longer on average [mean: 7.8 (95% CrI: 7.0, 8.6) days; SD: 5.2 (95% CrI: 4.7, 5.9) days];

whereas during the last 14 days (30 January to 13 February 2020), the serial intervals were much shorter on average [mean: 2.2 (1.5, 2.9) days; SD: 4.6 (4.1, 5.1) days]. Notably, the mean serial intervals were shortened by more than a factor of 3 over the 36-day period.

The transmission pair data also contain information for age, sex, household, and isolation delay (i.e., time duration from symptom onset to isolation) for most infectors. This allows for a granular stratification. Using either nonoverlapping or running time windows for data stratified by each of these factors, we find the same pattern of shorter serial intervals over time (Figs. 1B and 2A and tables S2 and S3). Therefore, we termed this changing serial interval the effective serial interval, which accounts for temporal changes caused by its potential driving factors. Notably, the length of effective serial intervals is positively associated with the length of isolation delay (Fig. 2A; figs. S5, S6, and S9; and tables S3 and S4), which accounts for the decreasing isolation delay over time (fig. S2). Therefore, early isolation (shorter than the median isolation delay) translates into shorter serial intervals [mean: 3.3 (2.7, 3.8) days; SD: 4.5 (4.1, 4.9) days], and de-

layed isolation (longer than the median isolation delay) is associated with longer serial intervals [mean: 6.8 (6.2, 7.3) days; SD: 5.3 (4.9, 5.7) days] (table S2). Stratification by age, gender, or household shows no clear differences in serial interval estimates. Our findings are robust to using alternative distributions (e.g., Gumbel distribution) for model fitting (fig. S11) and the infector-based approach (fig. S14).

Our probabilistic, individual-based simulated and regression models confirm that serial intervals are positively associated with isolation delay (section 5, supplementary materials). We found that the serial intervals become shorter on the basis of how much faster the infectors are isolated, regardless of when an infector starts to be infectious before symptom onset (fig. S5). In an individual-based simulation model with a mean generation time of 7.8 days, the simulated mean serial intervals are reduced from ~8.0 to ~1.2 days when the isolation delay is reduced from 10 to 0 days. We found through regression models that up to 51.5% of the variability in daily empirical serial interval can be explained by isolation delay and further improved by other NPI factors, which explain an additional 15.6 to 16.7% of the variability (table S5).

In practice, the time-varying serial interval may affect the estimation of epidemic parameters, including the transmissibility. The real-time transmissibility of an infectious disease is often characterized by the instantaneous reproduction number ( $R_t$ ), which is defined as the expected number of secondary infections caused by an infector on day  $t$ . The pathogen spreads when  $R_t > 1$  and is under control when  $R_t < 1$ . To examine the effect of serial intervals on  $R_t$ , we first obtained the daily number of cases on the basis of the onset dates of infectors and infectees among the 1407 transmission pairs (Fig. 2, B to D). By applying the statistical method developed by Cori *et al.* (28), we estimated  $R_t$  for each day during 20 January and 13 February 2020. We noticed substantial differences in estimates of  $R_t$  between using a single stable serial interval distribution and time-varying effective serial interval distributions. The magnitude of this difference is more prominent during the prepeak and postpeak periods than it is during the peak week when  $R_t \approx 1$  (Fig. 2, B to D).

We observed that the serial interval for COVID-19 in mainland China was shortened by more than a factor of 3 in the 36 days between 9 January and 13 February 2020. This reduction was driven by intensive NPIs, particularly the reduction of the isolation delay period. Isolation of an infector 1 day earlier is expected to reduce the mean serial interval by 0.7 days. Thus, the serial interval was shortened by >3 days if infectors were rapidly isolated (Figs. 1B and 2A and tables S2 and S3). This is consistent with advocating isolation of cases

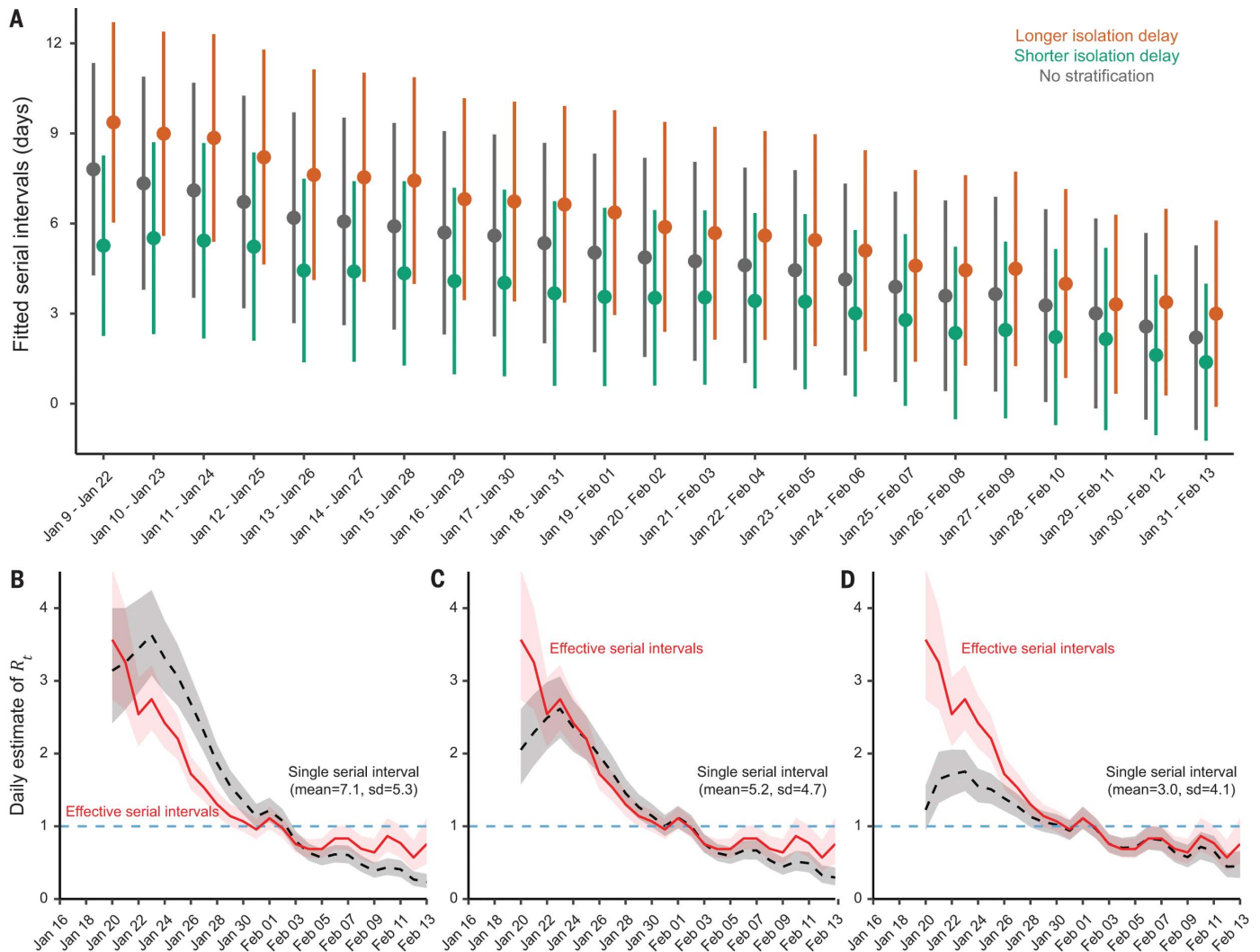


**Fig. 2. Real-time effective serial intervals and instantaneous reproduction number  $R_t$ .** (A) Estimated serial interval distribution for each 14-day running time window. Dark gray color indicates fitting data with no stratification, whereas green and orange indicate fitting data with isolation delay shorter and longer, respectively, than the median isolation delay of each running time window. Dots and bars indicate the estimated median and IQR, respectively. (B to D) Daily estimates of  $R_t$  by using real-time effective serial interval distributions [as in (A)]

versus using a single fixed serial interval distribution. Red curves and light pink shaded regions indicate the median and 95% CrI, respectively, of daily  $R_t$  estimated using real-time effective serial interval distributions. Black dashed curves and light gray shaded regions indicate the median and 95% CrI, respectively, of daily  $R_t$  estimated using a single serial interval distribution fixed, with a mean of 7.1 and SD of 5.3 days in (B), a mean of 5.2 and SD of 4.7 days in (C), and a mean of 3.0 and SD of 4.1 days in (D).

and quarantining contacts within 1 day from symptom onset, which has been estimated to reduce COVID-19 transmission by 60% (8). We have not identified any substantial effects of gender or age of infectors on serial interval, but the NPIs were found to be significant for the transmission in communities rather than in households (table S5). Other studies (15, 20) have estimated that the infectiousness of COVID-19 is greater at symptom onset. Although a short serial interval indicates that a substantial proportion of transmission events have occurred by the time symptoms are apparent (14), because of prolonged viral shedding (14, 29, 30) case isolation is still likely to reduce further transmission. Changes in the

serial interval can therefore indicate effective implementation of specific transmission-reduction measures.

There are some limitations to our work. First, it is possible that there was recall bias on the onset of first symptoms in the line-list data; however, given the centralized pandemic response in mainland China, we expected that recall bias would not affect our main conclusions (figs. S12 and S13). Second, other factors may have influenced the reduction of effective serial intervals, as we can only explain up to 72% of the variance in observed serial intervals. Finally, our current transmission pair data do not contain variables about the potential exposure window of each case, which do

not allow further inferences on the transmission potential.

Our results indicate that caution is needed when attempting to generalize estimates of the serial interval distribution to other places or to other periods of time in the same place, for example when estimating instantaneous reproductive numbers (Fig. 2, B to D). The real-time metric of effective serial intervals indicates that transmission models also need to account for the temporal variation in serial intervals as an epidemic proceeds. Effective serial intervals may provide better measurements of instantaneous transmissibility ( $R_t$ )—because they include the effects of possible drivers of transmission—and could be helpful

to policy-makers because they offer real-time information on the impact of public health measures.

## REFERENCES AND NOTES

- World Health Organization (WHO). "Coronavirus disease 2019 (COVID-19): Situation report – 162" (WHO, 2020); [www.who.int/docs/default-source/coronaviruse/situation-reports/20200629-covid-19-sitrep-161.pdf?sfvrsn=74fde64e\\_2](http://www.who.int/docs/default-source/coronaviruse/situation-reports/20200629-covid-19-sitrep-161.pdf?sfvrsn=74fde64e_2).
- M. U. G. Kraemer *et al.*, *Science* **368**, 493–497 (2020).
- C. Wenham, J. Smith, R. Morgan, Gender and COVID-19 Working Group, *Lancet* **395**, 846–848 (2020).
- J. M. Jin *et al.*, *Front. Public Health* **8**, 152 (2020).
- J. Hellewell *et al.*, *Lancet Glob. Health* **8**, e488–e496 (2020).
- L. Ferretti *et al.*, *Science* **368**, eabb6936 (2020).
- R. Armitage, L. B. Nellums, *Lancet Public Health* **5**, e256 (2020).
- R. M. Anderson, H. Heesterbeek, D. Klinkenberg, T. D. Hollingsworth, *Lancet* **395**, 931–934 (2020).
- J. R. Koo *et al.*, *Lancet Infect. Dis.* **20**, 678–688 (2020).
- K. Prem *et al.*, *Lancet Public Health* **5**, e261–e270 (2020).
- M. A. Vink, M. C. Bootsma, J. Wallinga, *Am. J. Epidemiol.* **180**, 865–875 (2014).
- J. T. Wu, K. Leung, G. M. Leung, *Lancet* **395**, 689–697 (2020).
- M. Chinazzi *et al.*, *Science* **368**, 395–400 (2020).
- H. Nishiura, N. M. Linton, A. R. Akhmetzhanov, *Int. J. Infect. Dis.* **93**, 284–286 (2020).
- H. Y. Cheng *et al.*, *JAMA Intern. Med.* 10.1001/jamainternmed.2020.2020 (2020).
- Z. Du *et al.*, *Emerg. Infect. Dis.* **26**, 1341–1343 (2020).
- Q. Li *et al.*, *N. Engl. J. Med.* **382**, 1199–1207 (2020).
- J. M. Griffin *et al.*, *medRxiv* 2020.05.08.20095075 [Preprint]. 11 May 2020. <https://doi.org/10.1101/2020.05.08.20095075>.
- S. Ma *et al.*, *medRxiv* 2020.03.21.20040329 [Preprint]. 24 March 2020. <https://doi.org/10.1101/2020.03.21.20040329>.
- X. He *et al.*, *Nat. Med.* **26**, 672–675 (2020).
- Q. Bi *et al.*, *Lancet Infect. Dis.* **20**, 911–919 (2020).
- J. Zhang *et al.*, *Science* **368**, 1481–1486 (2020).
- Lin, PDGLin/COVID19\_EffSerialInterval\_NPI: Serial interval of SARS-CoV-2 was shortened over time by non-pharmaceutical interventions, version v1.0, Zenodo (2020); <https://doi.org/10.5281/zenodo.3940300>.
- H. Tian *et al.*, *Science* **368**, 638–642 (2020).
- K. Leung, J. T. Wu, D. Liu, G. M. Leung, *Lancet* **395**, 1382–1393 (2020).
- A. Pan *et al.*, *JAMA* **323**, 1915–1923 (2020).
- J. Zhang *et al.*, *Lancet Infect. Dis.* **20**, 793–802 (2020).
- A. Cori, N. M. Ferguson, C. Fraser, S. Cauchemez, *Am. J. Epidemiol.* **178**, 1505–1512 (2013).
- L. Zou *et al.*, *N. Engl. J. Med.* **382**, 1177–1179 (2020).
- Y. Pan, D. Zhang, P. Yang, L. L. M. Poon, Q. Wang, *Lancet Infect. Dis.* **20**, 411–412 (2020).

## ACKNOWLEDGMENTS

We thank all the health workers and volunteers who collected data throughout the COVID-19 outbreak. We thank H. Salje, S. Cauchemez, L. A. Meyers, J. Paireau, Q. Bi, B. Yang, X. Liu, and L. Hu for discussions. **Funding:** We acknowledge financial support from the Health and Medical Research Fund, Food and Health Bureau, Government of the Hong Kong Special Administrative Region, China (grant no. COVID190118); the Investissement d'Avenir program, the Laboratoire d'Excellence Integrative Biology of Emerging Infectious Diseases program (grant no. ANR-10-LABX-62-IBEID); the European Research Council (grant no. 804744); the European Union's Horizon 2020 research and innovation program under grant agreement no. 101003589 (RECOVER); the National Institutes of Health (no. U01 GM087719); the Open Fund of Key Laboratory of Urban Land Resources Monitoring and Simulation, Ministry of Land and Resources, China (no. KF-2019-04-034); the National Natural Science Foundation of China (nos. 61773091, 11875005, 61976025, and 11975025); and a University of Cambridge COVID-19 Rapid Response Grant. S.T.A. acknowledges

the research computing facilities and advisory services offered by Information Technology Services, The University of Hong Kong. L.W. acknowledges the computational and storage services provided by the IT department at the Institut Pasteur. **Author contributions:** L.W., S.T.A., E.H.Y.L., and B.J.C. conceived the study, designed the statistical and modeling methods, conducted analyses, interpreted results, and wrote and revised the manuscript. X.-K.X., Z.D., and Y.W. collected and compiled data, interpreted results, and revised the manuscript. G.M.L. supervised the study, interpreted results, and revised the manuscript. **Competing interests:** B.J.C. reports honoraria from Sanofi Pasteur and Roche. The authors report no other potential conflicts of interest. **Data and materials availability:** All data and codes are available in the main text, the supplementary materials, or Zenodo (23). This work is licensed under a Creative Commons Attribution 4.0 International (CC BY 4.0) license, which permits unrestricted use, distribution, and reproduction in any medium, provided the original work is properly cited. To view a copy of this license, visit <https://creativecommons.org/licenses/by/4.0/>. This license does not apply to figures/photos/artwork or other content included in the article that is credited to a third party; obtain authorization from the rights holder before using such material.

## SUPPLEMENTARY MATERIALS

[science.sciencemag.org/content/369/6507/1106/suppl/DC1](https://science.sciencemag.org/content/369/6507/1106/suppl/DC1)  
Materials and Methods  
Figs. S1 to S14  
Tables S1 to S5  
References (31–49)  
MDAR Reproducibility Checklist

[View/request a protocol for this paper from Bio-protocol.](#)

20 May 2020; accepted 13 July 2020  
Published online 21 July 2020  
10.1126/science.abc9004